



ELSEVIER

Contents lists available at [SciVerse ScienceDirect](http://www.sciencedirect.com)

Comptes Rendus Chimie

www.sciencedirect.com

Full paper/Mémoire

Antioxidant and antimicrobial activities of green tea extract loaded into nanostructured lipid carriers



Ana-Maria Manea*, Bogdan Stefan Vasile, Aurelia Meghea

Faculty of Applied Chemistry and Materials Science, University Politehnica of Bucharest, Polizu Street No 1, 011061 Bucharest, Romania

ARTICLE INFO

Article history:

Received 13 May 2013

Accepted after revision 25 July 2013

Available online 28 August 2013

Keywords:

Nanostructured lipid carriers

Green tea extract

High shear homogenization

Antioxidant activity

Antibacterial activity

ABSTRACT

In this paper, the preparation and characterization of some novel nanostructured lipid carriers for drug delivery are reported. They are obtained by mixing two solid lipids, cetyl palmitate and glyceryl stearate, with three types of vegetable oils: grape seed oil, St. John's wort oil (*Hypericum perforatum* oil) and sea buckthorn oil. In order to increase their antioxidant and antimicrobial properties, they are co-loaded with green tea extract by using a modified high shear homogenization technique. Size distribution and polydispersity index of the developed nanostructured lipid carriers determined by the dynamic light scattering, and corroborated with the results obtained by the transmission electron microscopy analysis, confirmed that the structures obtained are at nanoscales. The crystallinity behavior of the prepared nanostructured lipid carriers has been studied by differential scanning calorimetry; zeta potential measurements show that all loaded nanostructures present excellent physical stability. Their antioxidant and antimicrobial properties evaluated by an appropriate in vitro analysis using the chemiluminescence method, and the diffusion disc method, respectively, show that green tea extract could be utilized as a valuable natural source of antioxidant and antimicrobial agent. These new nano-formulations proved to have significant potential for nutritional and pharmaceutical applications.

© 2013 Académie des sciences. Published by Elsevier Masson SAS. All rights reserved.

1. Introduction

Results of many researches developed on the health benefits of green tea for a wide variety of applications, including different activities, such as antimicrobial [1], antioxidant [2], antiviral [3], and anti-mutagenic [4] activities, are already available. In the past few years, special attention has been paid to the antioxidant activities of the polyphenolic compounds present in green tea due to their pharmaceutical properties. The performed studies report that green tea extract (GTE) shows many health beneficial properties, particularly against the damage

caused by pollution, stress, cigarette smoke and other toxins [5], prevention of cardiovascular diseases [6], cancer [7–9], diabetes [10].

The beneficial health effects of green tea have been attributed to the presence of antioxidants that act as receptors of free radicals. Green tea is an excellent source of polyphenols, which are natural antioxidants that can be used as alternatives to synthetic antioxidants, as they are typically less harmful and appear to have an equivalent effect upon the inhibition of oxidation [11]. These antioxidants, which inhibit oxidation of organic molecules, are very important, not only for living systems, but also for food preservation [12]. There are several polyphenol catechins present in GTE, such as epicatechin (EC), epicatechin-3-gallate (ECG), epigallocatechin (EGC), and epigallocatechin-3-gallate (EGCG), with beneficial effects on health [13]. Fig. 1 presents the chemical structure of these polyphenols.

* Corresponding author.]

E-mail addresses: am_manea@yahoo.com, anamariamanea1602@gmail.com (A.-M. Manea).

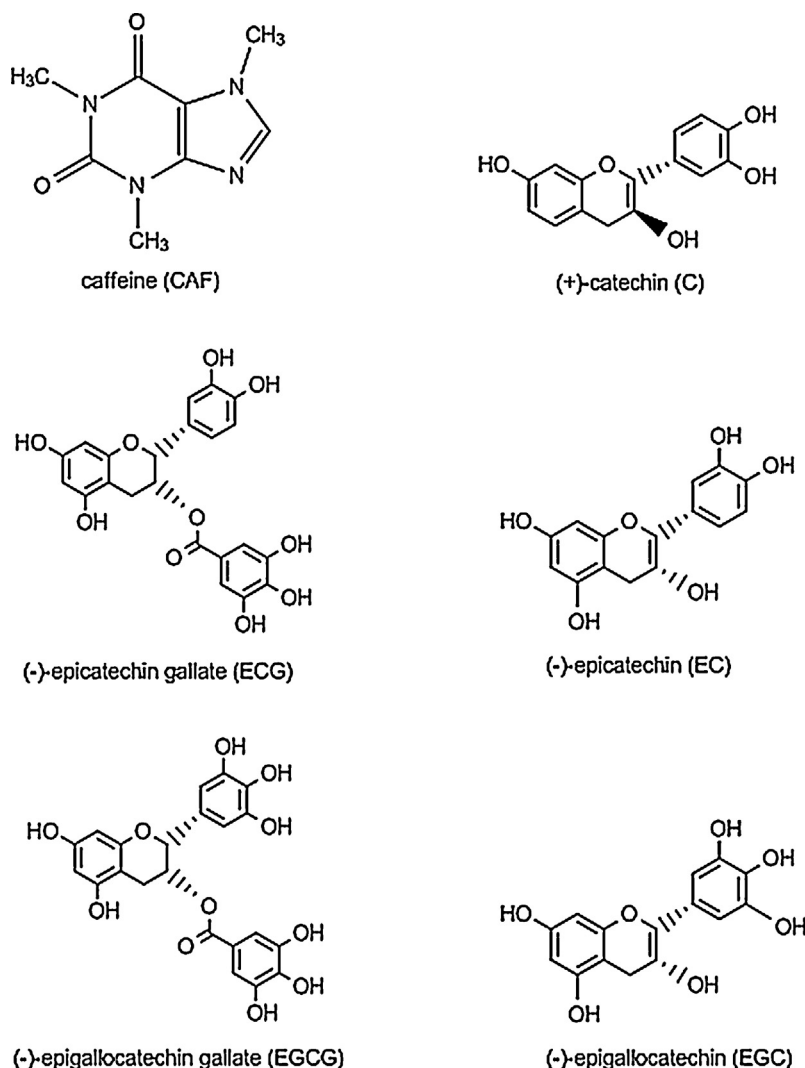


Fig. 1. Chemical structures of common bioactive molecules present in green tea extract.

Synthetic chemicals are often used as antimicrobials in food processing and storage to eliminate the food-borne pathogens, many of which contributing to increase the resistance to antibiotics and having side adverse effects, even carcinogenic.

It is generally known that current research in the field of targeting drug delivery systems is focusing on the development and marketing of nanomaterials for both passive and active targeting. Among the first developed delivery systems are liposomes, which are considered to be adequate for encapsulation of both hydro- and liposoluble compounds, and to control their delivery rate, degradation and bioavailability [14–16]. Liposomes exhibit a series of advantageous effects, for instance for direct administration in tissues associated with reticuloendothelial system, as auxiliaries in vaccine formulations, etc. However, formulations based on liposomes have numerous weak points related to complex and rather expensive preparation conditions, difficulties

during sterilization, low stability on storage, limitations caused by low capacity of solubilization of hydrophobic drugs and in drug delivery control. In contrast, the new drug delivery systems for topical medications, such as solid lipid nanoparticles (SLNs) and nanostructured lipid carriers (NLCs), have demonstrated to enhance follicular targeting, to allow high concentrations of the active drug and to penetrate the skin [17], to allow controlled release and gradual distribution of therapy compounds.

As referring to antioxidant compounds encapsulated, attempts have been made in the recent past by several researchers toward effective topical delivery of retinoids by employing various vesicular and non-vesicular carriers, like liposomes and mixed vesicles [18], nanocapsules [19] and lipid nanoparticles. In this context, new types of nanostructured lipid carriers containing natural oils as matrix components and cetyl palmitate and glyceryl stearate as safe accepted surfactants [20] could be developed for encapsulating green tea extract

in order to confer enhanced antioxidant and antimicrobial activities.

The aim of the present study is the preparation and characterization of GTE-loaded nanostructured lipid carriers by using a versatile high shear homogenization (HSH) technique that avoids the use of organic solvents, as in other techniques. GTE-loaded NLCs with three types of vegetable oils are obtained, containing grape seed oil (GSO), St. John's wort oil (HPO) and sea buckthorn oil (SBO), which confer enhanced antioxidant properties and significant antimicrobial activity.

2. Materials and methods

2.1. Materials

The composition of the GTE used consists of polyphenols (51.8% determined by UV), catechins (39.2%) and caffeine (9.8%) determined by HPLC. The catechins present in GTE are: EGC (9.5%), DL-C (1.92%), EG-GG (15.5%), EC (3.8%), GCG (2.6%), ECG (5.9%). The other materials used in this study, such as polyethylene glycerol sorbitan monolaurate (Tw20), polyethylene glycol sorbitan monooleate (Tw80), were purchased from Merck (Germany). Synperonic PE/F68 (block copolymer of polyethylene and polypropylene glycol), $\text{l-}\alpha$ -phosphatidylcholine (lecithin) and tris[hydroxymethyl] aminomethane (luminol) were purchased from Sigma–Aldrich Chemie GmbH (Munich, Germany). *n*-Hexadecyl palmitate (CP) 95% was purchased from Acros Organics (USA), while glycerol stearate (GS) was supplied by Cognis GmbH. Grape seed oil was purchased from S.C. Manicos SRL (Romania). St. John's wort oil (*Hypericum perforatum* oil) was purchased from Solaris and sea buckthorn oil was provided by Hofigal (Romania). A spectroscopic-quality ethanol (Sigma–Aldrich) was used as the solvent.

2.2. Preparation of NLC

The GTE-loaded NLCs were prepared by a modified HSH method, which has been previously described [21]. Briefly, the HSH method consists of the production of NLCs by preparing two different surfactant phases, lipid and aqueous obtained separately. The lipid phase consisted of CP, GS and GSO or HPO or SBO and the aqueous surfactant phase of Synperonic F68, Tw20 or Tw80, lecithin and double-distilled water. They were heated to the same temperature of 85 °C for 30 min. To the lipid phase, various amounts of GTE were added. Before mixing the two phases, the aqueous surfactant phase was stirred for 2 min at high speed (15 000 rpm). Then, a pre-emulsion was produced by high shear stirring and processed by HSH. Trehalose at the concentration of 5 wt% was used in the freeze-drying process as the cryoprotector. NLCs suspensions were frozen in an aqueous trehalose solution at –25 °C for 24 h, and then, the samples were transferred to the freeze-dryer at –55 °C for 72 h. After that, the NLCs powders were collected for further experiments. The obtained lyophilized samples exhibit a powdery aspect.

2.3. Particle size and zeta potential measurements

Nanostructured lipid carriers were characterized for their size, average diameter (Zave) and the polydispersity index (PdI) by dynamic light scattering (DLS) with a Zetasizer Nano ZS (Malvern Instruments Ltd.), at 25 °C under an angle of 90°. The particle size measurements were performed on the day of production. All the samples were diluted in deionized water to an adequate scattering intensity prior to the measurement. Each measurement was performed in triplicate and both Zave and PdI were determined.

The zeta potential (ZP) was measured using the same Zetasizer of Malvern Instrument. The electrophoretic mobility was converted into ZP by using the Helmholtz–Smoluchowski equation. The ZP measurements were performed in deionized water with the conductivity adjusted to 50 $\mu\text{S}/\text{cm}$ by the addition of a sodium chloride solution (0.9% w/v).

2.4. Transmission electron microscopy (TEM) examination

The transmission electron micrographs were obtained by using a 300 kV Tecnai G² F30 S-TWIN transmission electron microscope equipped with STEM with a HAADF detector, EDX, EELS. The samples were prepared by depositing a drop of NLCs dispersion onto a 400-mesh holey carbon-coated copper grid. After that, a 15% wolfram solution was sprayed onto the grid and left to dry for 24 h prior to the analysis.

2.5. UV–Vis analysis

The UV–Vis absorption spectra of lyophilized NLCs–GTE were recorded in the wavelength range 220–2200 nm using a Jasco double-beam V670 spectrophotometer. The diffuse reflectance analysis was performed with the ILN-725 device endowed with an integrating sphere. The lyophilized samples were prepared in the form of pellets in the presence of MgO, which has been also used as a reference.

2.6. Differential scanning calorimetry analysis

Differential scanning calorimetry (DSC) measurements were performed using a DSC 204 F1 apparatus (Netzsch). Approximately, 10 mg of lipid bulk material or equivalent NLCs dispersion were inserted into an aluminum pan and sealed hermetically. It was heated from 25 °C to 100 °C at a rate of 5 °C/min. The crystallinity index (Ci) was calculated using the following equation:

$$Ci = \frac{\Delta H_{\text{NLC}}[\text{J/g}]}{\Delta H_{\text{bulk}}[\text{J/g}]C_{\text{lipid phase}}} \times 100\% \quad (1)$$

where ΔH_{NLC} is the enthalpy of NLC; ΔH_{bulk} the enthalpy of the bulk; $C_{\text{lipid phase}}$ the concentration of the lipid phase.

2.7. Antioxidant activity

The antioxidant activity (AA) of free NLCs and NLCs–GTE was determined and compared with that of GTE by the

chemiluminescence method (CL) using a Chemiluminometer Turner Design TD 20/20, USA. A cyclic hydrazide (luminol) was used as the light-amplifying substance. Luminol increases the detection sensitivity of activated oxygen species in the sample [22]. H₂O₂ was used as a generator system for free radicals in a buffer Tris–HCl solution with a pH = 8.6. The antioxidant activity of ethanol solutions of green tea and ethanol solutions of lyophilized NLCs–GTE with the same concentration of active compound was calculated using the following equation:

$$AA = \frac{I_0 - I_s}{I_0} \times 100\% \quad (2)$$

where I_0 is the maximum CL of standard at $t = 5$ s; I_s is the maximum CL of the sample at the same time ($t = 5$ s).

2.8. Antibacterial activity

The antibacterial activity of free NLC, NLCs–GTE and GTE alone were tested against the action of *Escherichia coli* K 12-MG1655. The antibacterial activity measurements were performed by the agar well diffusion method [23].

The bacterial strains were grown in Luria Bertani Agar (LBA) plates at 37 °C with the following medium composition: peptone: 10 g/L; yeast extract: 5 g/L, NaCl: 5 g/L and agar: 20 g/L. The stock culture was maintained at 4 °C. All the bacteria-containing plates were incubated at 37 °C for 24 h.

The antibacterial activity of the microorganisms with free NLCs, NLCs–GTE and GTE alone was determined by measuring the size of the inhibition zone (IZ, mm) as a clear, distinct zone of inhibition surrounding agar wells. The reported results are average values of three experiments and are given with the standard deviation (SDs).

3. Results and discussion

3.1. Particle size

Evaluation of NLCs' size distribution was achieved in optimized systems type Tw20 or Tw80/lecithin/copolymer block, depending on the encapsulated GTE concentrations and on the type of vegetable oil used in the formation of the lipid matrix. Fig. 2 illustrates the particle size distribution of three NLCs–GTE series of samples prepared with GSO, HPO, and SBO oils, respectively. The compositions of all free NLCs and GTE-loaded NLCs samples are given in Table 1.

Concerning the effectiveness of the three types of vegetable oils used, one may observe that the lipid matrix prepared with GSO (Fig. 2a) exhibits the smallest average particle diameter for the free lipid matrix of Zave = 125.6 nm, while for the two other ones prepared with HPO and SBO relative higher values are obtained.

As a first observation, one can notice that both size and Pdl of NLCs are increasing with the GTE content for all the three types of vegetable oils used and are higher when Tw80 was used as the surfactant, as compared to Tw20 (Table 1). Moreover, the low values observed for Pdl, ranging between 0.15 and 0.30, reveal a good degree of homogeneity for all the systems investigated, with a similar increasing tendency for Tw80 as compared to Tw20 and with increasing the green tea content.

As limit values, the smallest average particle diameter size was obtained when using GSO as the vegetable oil, Tw20 as a main non-ionic surfactant and a concentration of 0.1 wt% of GTE (Zave = 145.1 nm; Pdl 0.203), while the largest diameter (Zave = 317.2 nm and Pdl 0.294) was obtained for SBO, Tw80 as a surfactant and a concentration of 0.17 wt% of GTE.

Table 1
Composition and physico-chemical characterization of free NLCs and NLCs–GTE.

Sample	Composition ^a			ZP (mV)	DSC characteristics	
	GTE (%)	Main surfactant ^b	Oil type		C.I.	P.t./shoulder (°C)
Free NLC1	–	Tw20	GSO	–37.8 ± 1.87	63.85	50.4
NLC–GTE1	0.1	Tw20	GSO	–42.8 ± 0.404	–	–
NLC–GTE2	0.17	Tw20	GSO	–30.5 ± 0.808	79.49	49.1/58
Free NLC2	–	Tw80	GSO	–33.9 ± 1.63	–	–
NLC–GTE3	0.1	Tw80	GSO	–35.8 ± 0.608	–	–
NLC–GTE4	0.17	Tw80	GSO	–22.6 ± 2.25	82.26	50.1
Free NLC3	–	Tw20	HPO	–55.3 ± 0.721	–	–
NLC–GTE5	0.1	Tw20	HPO	–42.1 ± 1.00	79.99	–
NLC–GTE6	0.17	Tw20	HPO	–43.7 ± 0.551	76.53	49.4
Free NLC4	–	Tw80	HPO	–57.9 ± 0.361	92.36	49/57.5
NLC–GTE7	0.1	Tw80	HPO	–41.1 ± 0.60	83.33	–
NLC–GTE8	0.17	Tw80	HPO	–37.6 ± 1.06	88.07	49.1/41.1/55.9
Free NLC5	–	Tw20	SBO	–44.7 ± 0.819	76.05	50.5/59.5
NLC–GTE9	0.1	Tw20	SBO	–44.6 ± 0.643	–	–
NLC–GTE10	0.17	Tw20	SBO	–46.4 ± 0.520	82.83	51/58.2
Free NLC6	–	Tw80	SBO	–40.5 ± 0.473	–	–
NLC–GTE11	0.1	Tw80	SBO	–47.5 ± 0.624	–	–
NLC–GTE12	0.17	Tw80	SBO	–54.6 ± 1.91	89.36	49.1

^a All NLCs samples were prepared with 10% (w/w) lipid mixtures, in a ratio of CP:GS:GSO/HPO/SBO = (1.16:1.16:1).

^b A mixture of 1% of Lecithin:SynperonicF68 (1:1) was added to the main non-ionic surfactant.

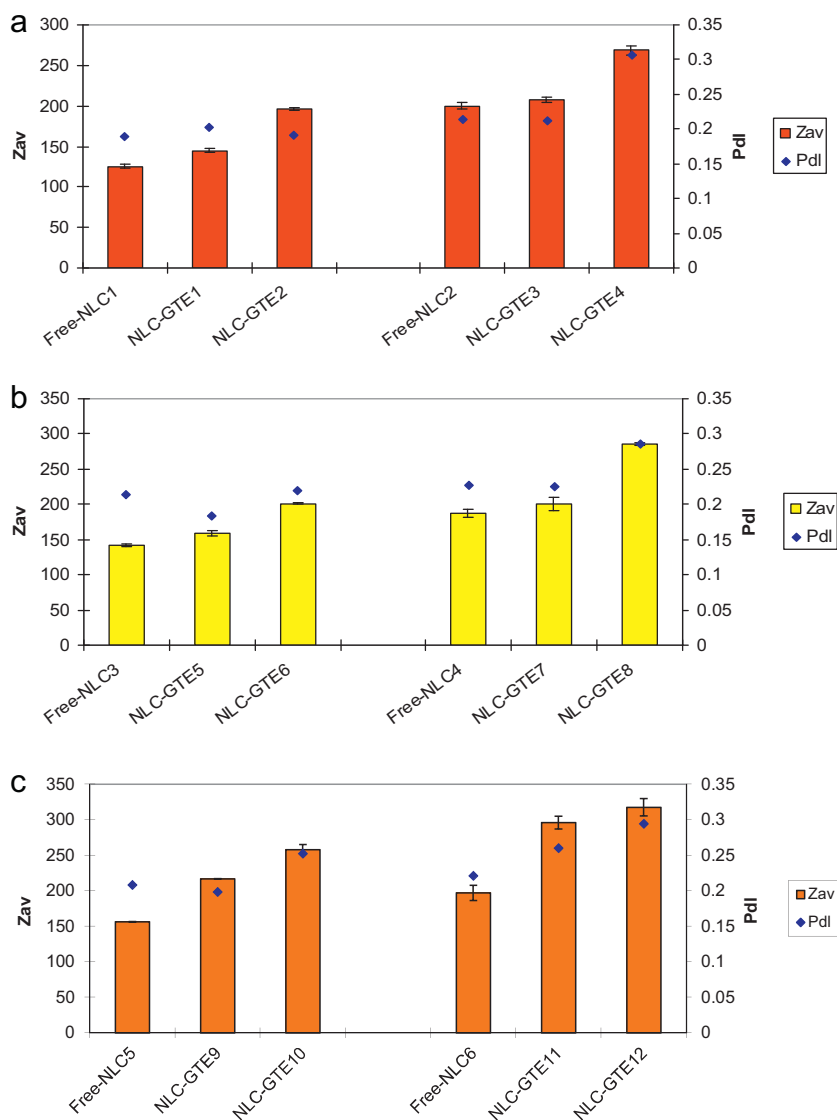


Fig. 2. Dynamic light scattering (DLS) dimensional analysis of NLCs-GTE systems prepared with different oils: GSO (a), HPO (b) and SBO (c).

These size evaluations were confirmed by transmission electron microscopy (TEM) analysis, as will be discussed later.

3.2. Zeta potential

The lipid nanodispersion stability analysis, based on electrokinetic potential values, revealed that all the NLCs-GTE samples (except NLC-GTE4) show excellent physical stability. The measured values of the electro-negative potential are ranging between -30 mV and -58 mV [24,25] (Table 1).

Concerning the types of vegetable oils used for obtaining lipid matrices, the trend of increasing stability is in the order: GSO/HPO/SBO and also from Tw80 to Tw20 in the case of GSO, HPO oils, but it is the reverse for SBO-loaded nanoparticles.

A detailed analysis of zeta potential values obtained with different compositions variants highlights some systematic changes, which allow us to differentiate between the contributions of co-loaded oil extracts. Indeed, when comparing the stability of free NLCs with that of loaded NLCs, it is increasing for GSO in case of low GTE content (0.1 wt%), while decreasing in case of higher GTE content (0.17 wt%) for both surfactants used, thus, arriving to the minimum absolute ZP value (-22.6 mV) for NLC-GTE4 for Tw80, corresponding to a rather medium stability.

In the case of the HPO extract, there is a significant decrease in ZP values by 15–20 mV, without having a noticeable influence of GTE content or a surfactant used. Nevertheless, all the systems remained in a high-level range of stability. When the SBO extract was used, the loaded NLCs show in all the cases quite similar or higher stability as compared to free NLCs.

This behavior suggests that in the case of the HPO, and particularly of the GSO extract, by increasing the GTE content, the loading capacity of the lipidic matrix is exceeded, and thus, the stability of the system is diminished. This conclusion is supported by a comparative analysis using DSC, which shows that the nanoparticles prepared with GSO and a concentration of 0.17 wt% GTE undergo a rearrangement of the lipid network, which led to the more ordered grid and, as a result, a potential expulsion of the active substance.

On the contrary, for the SBO extract, the stability of loaded NLCs is significantly higher as compared to free NLCs, which can be interpreted by a better compatibility between GTE and SBO components, and thus, a more favorable accommodation of both oils into the lipidic matrix is possible.

3.3. Transmission electron microscopy (TEM)

Representative TEM images of NLCs prepared with the three types of vegetable oils and Tw20 used as a main non-ionic surfactant loaded with 0.17 wt% GTE are shown in Fig. 3.

One can observe that the particles have a spherical shape that does not depend on the type of oil used. The average diameter sizes of these particles range between 195 nm and 257 nm. This observation confirms a less ordered crystalline structure of the lipid phase (α -form of crystallization), knowing that an ordered structure (β -form) is characteristic for elongated crystals [26,27]. Prevention of the β -conformation is desirable, because it is associated with the expulsion of the encapsulated active component [28]. This observation is also confirmed by DSC analysis. The particles sizes of the different formulations were in accordance with the obtained DLS data (Fig. 2).

3.4. UV–Vis spectroscopy

Their chemical composition, rich in polyphenols specific to the oil extracts co-loaded in the studied lipidic matrices, confers to various NLCs particular fingerprints in UV–Vis spectra, which are very useful in assessing their incorporation, even at the nanoscale. Indeed, GTE components absorb strongly in the UV–visible domain. Therefore, the UV–Vis reflectance spectra represent a clear evidence of GTE presence into NLCs prepared with the three vegetable oils. Since the GTE stability is a basic condition to maintain its properties, in order to observe its presence and stability after encapsulation, the electronic spectra of GTE-loaded NLCs, free NLCs and GTE alone have been compared.

The electronic spectra of GTE in the bulk show a strong absorption throughout the visible range, with maximum absorbance at 312–364 nm doublets. This confers to powder a yellowish color, originating from polyphenolic molecules. The absorption is extending towards higher wavelength and then, with a significant absorption at 488 nm, which arises from quinone molecules. These bands are visible also in the absorption spectra of the sample with GTE encapsulated, NLC–GTE2 (Fig. 4a). The absorption band

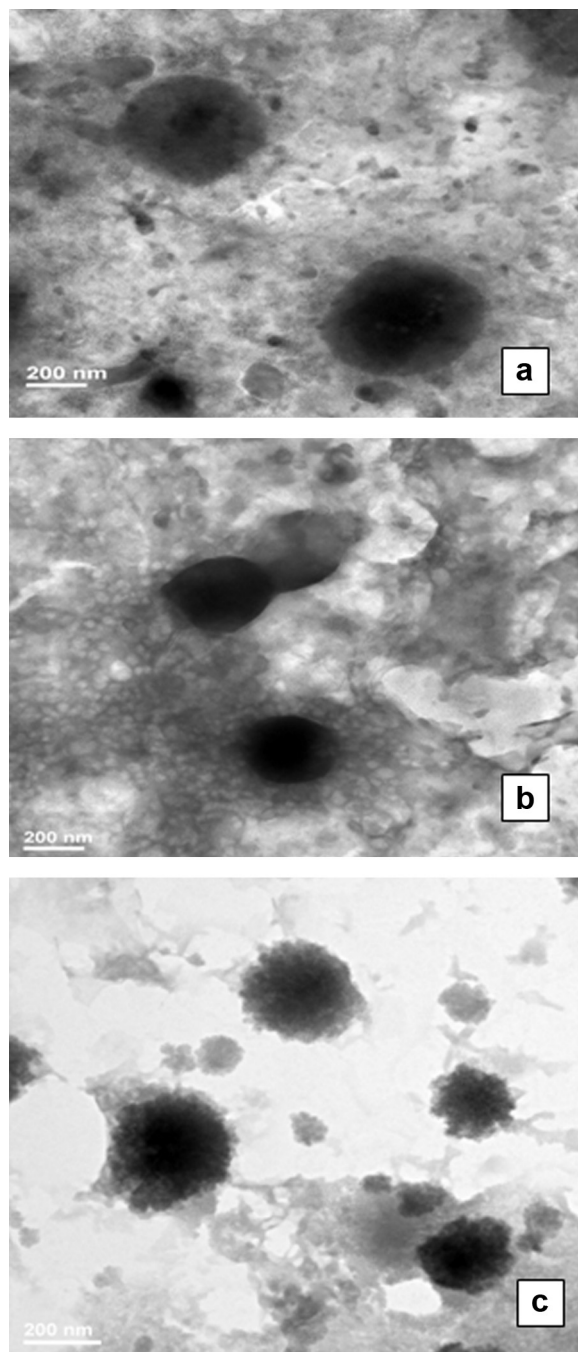


Fig. 3. Transmission electron microscopy image of NLC–GTE2 prepared with GSO (a); NLC–GTE6 prepared with HPO (b); NLC–GTE10 prepared with SBO (c).

at 312 nm is shifted in the sample NLC–GTE2 at 280 nm, clearly evidencing the n - π^* bands of phenolic molecules, while in the visible domain a significant shoulder at 366 nm remains.

The free NLC1 sample exhibits a peak in the UV range at 248 nm, with a shoulder at 268 nm attributable to the double bonds from the structure of unsaturated acids (oleic, linoleic). The shoulder at 268 nm may be a

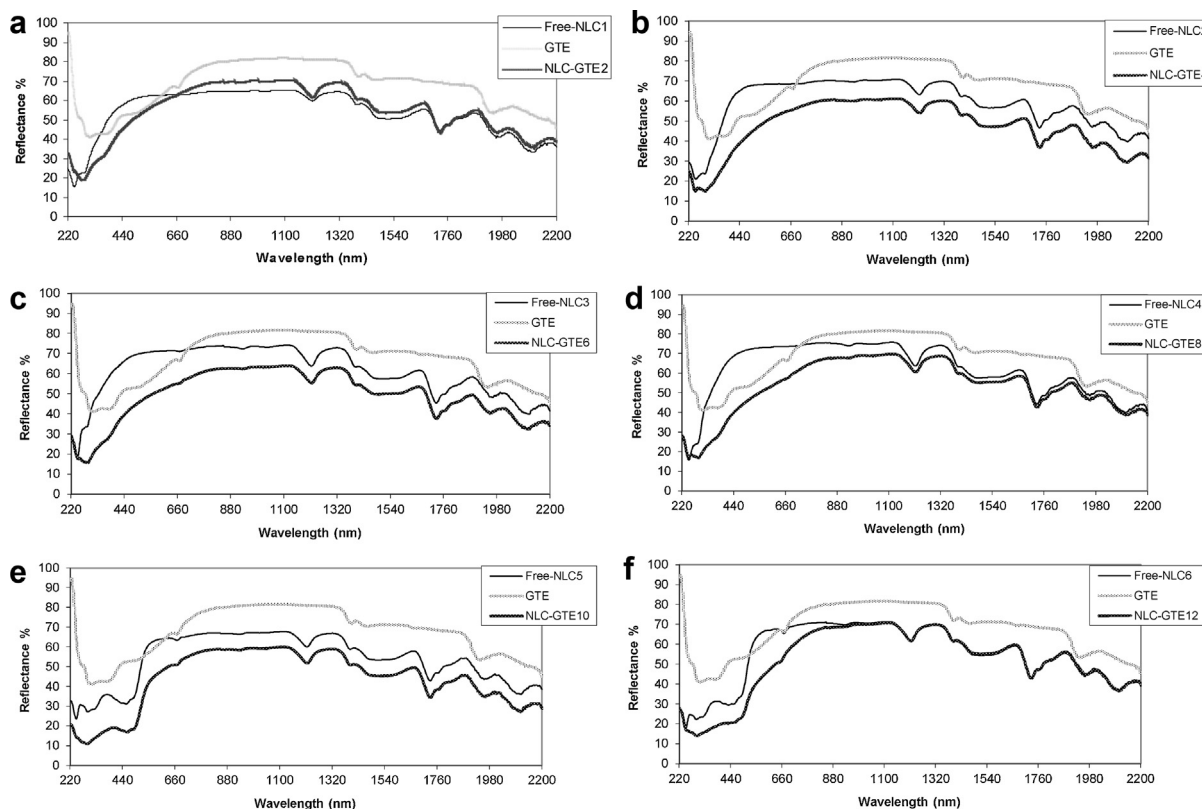


Fig. 4. UV-Vis absorption spectra of NLCs loaded with GTE.

contribution of the phenolic structure of tocopherol as one of the major components of GSO.

In a similar sample, free NLC2 (Fig. 5b), prepared with a more voluminous surfactant Tw80, the absorption spectrum of the sample conserves the main character of the lipid matrix. However, an inversion of the band intensities at 258 nm and 282 nm is observed, accompanied by their slight red shift to 260 nm and 284 nm (Fig. 4b). At the same time, the visible part of the spectrum is enlarged due to the contribution of the quinone band at 488 nm from native GTE. Thus, we can conclude that the use of Tw80 decreases the amount of encapsulated GTE into the lipid matrix, while a portion of this oil is expelled outside the lipid matrix.

In the sample prepared with HPO (Fig. 4c), the presence of this co-loaded oil is manifested by the shoulder at 310 nm, which by the extension band toward visible range confers on it a yellowish tint. In the sample of NLC co-loaded with GTE and HPO (NLC-GTE6), the presence of GTE is clearly evidenced by the band at 288 nm shifted to 312 nm and that at 374 nm shifted to 364 nm, respectively.

In a similar sample, free NLC4 (Fig. 4d), prepared with a more voluminous surfactant Tw80, one observes some bathochrom shifts in the lipid matrix from 250 nm to 242 nm, and from 300 nm to 288 nm, respectively. Also, some minor changes in intensities and widths of the specific bands of green tea can be seen in the NLC-GTE8 (Fig. 4d) sample.

In the sample free NLC5 (Fig. 4e) prepared with SBO, its presence is clearly evidenced by the intense band at 446 nm. The encapsulation of GTE in the lipid matrix is also highlighted by the presence of a band in the visible range, with a maximum absorption at 452 nm. Its position is intermediate between the shoulder at 488 nm, originating from GTE and the band from SBO at 446 nm. In addition, the contribution of the band at 446 nm from GTE decreases the absorption intensity at 446 nm of the encapsulated sample NLC-GTE10 (Fig. 4e).

The replacement of Tw20 surfactant by Tw80 in the free NLC6 sample (Fig. 4f) brings a slight modification of SBO absorption band in the visible range at 446–438 nm in the lipid matrix. There are also some changes observed for the bands of encapsulated GTE, with some bathochrom shifts from 286 nm (sample NLC-GTE10) to 298 nm (sample NLC-GTE12) and from 452 nm to 466 nm, respectively. Also in this case, the changes can be assigned to the steric effects manifested in the lipid matrix prepared with a more voluminous alkyl substituent Tw80.

3.5. DSC measurements

After crystallization, the particles may undergo different polymorphic transitions, which are mainly determined by the type of lipid constituents [29]. The lipid crystalline structure is generally correlated with the encapsulation of the active component. As NLCs pass from a less ordered to a more ordered solid state, an undesired phenomenon

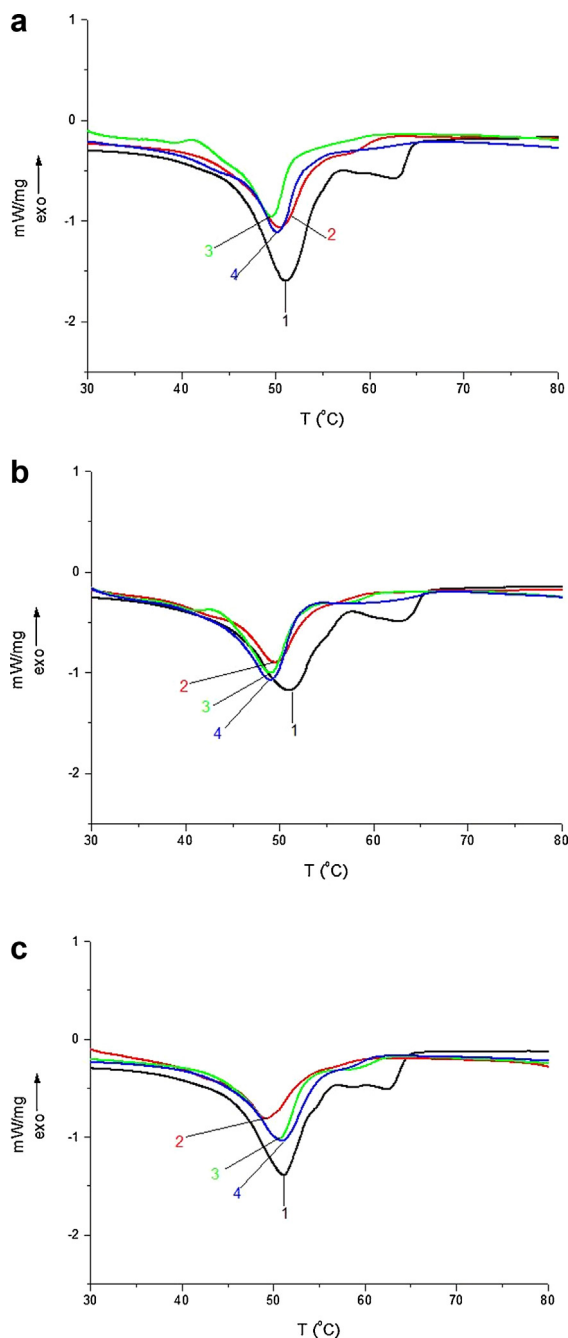


Fig. 5. Differential scanning calorimetry (DSC) curves for the lyophilized GTE-NLCs, compared with free NLCs and physical lipid mixture: a: NLCs prepared with GSO (1–Bulk, 2–NLC–GTE2, 3–NLC–GTE4, 4–free NLC1); b: NLCs prepared with HPO (1–Bulk, 2–NLC–GTE6, 3–NLC–GTE8, 4–free NLC4); c: NLCs prepared with SBO (1–Bulk, 2–NLC–GTE10, 3–NLC–GTE12, 4–free NLC5).

occurs, i.e. a sudden release of the active components. Therefore, it is essential to check the solid lipid status and polymorphism of NLCs [30].

The GTE-loaded NLCs samples prepared with the three types of vegetable oils show a similar endothermic behavior in an appropriate temperature range. It indicates

that the type of vegetable oils used does not lead to significant changes in the lipid network.

In the temperature range 30–80 °C, the presence of a main endothermic peak around 49–51 °C was observed, accompanied by a shoulder at 57–59 °C. The peak is mainly attributed to the solid lipid CP and GS, while the shoulder is a result of the presence of GSO, HPO or SBO extracts.

The endothermic curve at temperatures below 60 °C suggests the presence of different less ordered lipid crystalline phases. This behavior was expected because of the complex lipid mixture used to prepare the carrier matrix. We consider that obtaining an ordered crystalline structure is unlikely because of the increased number of liquid lipid components, and thus, their chemical heterogeneity can be considered as an advantage.

By comparing the DSC curves of GTE-loaded NLCs samples, free NLCs and physical lipid mixture as bulk (Fig. 5a–c), the following statements can be made:

- the presence of tensioactive surfactants confers to the lipid network an ordered arrangement, as it can be seen from the narrowing of the temperature melting range in case of NLCs samples compared to the physical mixture of solid and liquid lipids;
- melting temperatures of the GTE-loaded NLCs samples are shifted approximately by 1 °C with respect to those of free NLCs, indicating a disturbance of the lipid matrix and a slight increase in the particle size diameter. Moreover, by comparing the GTE-loaded NLCs with free NLCs, it was observed that GTE incorporation into solid lipid matrix results in a decrease of crystalline arrangement, underlined by a low intensity of the endothermic peak. This fact was observed for all vegetable oils used (Fig. 5a–c);
- the GTE-loaded NLCs prepared with Tw20 surfactant and with GSO (Fig. 5a) show a similar lipid arrangement with that of free NLCs. On the other hand, the loaded NLCs prepared with Tw20 indicate a less ordered crystalline arrangement. The intensity of endothermic peak decreases in comparison with that of free NLCs.

3.6. Antioxidant activity

The beneficial effect of GTE on the health is widely recognized due to its antioxidant properties [31].

In all tested samples (Fig. 6a–c), the antioxidant activity (AA) of NLCs–GTE was enhanced in comparison with that of pure GTE. The biggest difference was observed at low concentrations of GTE. By increasing the GTE content, we noticed a small increase of the AA of NLCs–GTE for both types of surfactants and for all the three kinds of vegetable oils used. There is only a small difference in the AA of NLCs–GTE samples prepared with the two surfactants types. This is also true for the three types of vegetable oils.

The first explanation for the antioxidant behavior revealed by NLCs–GTE samples was assigned to the average size and the GTE encapsulation effect. However, taking into account the antioxidant properties of the three types of vegetable oils used, the AA of free NLCs should be also taken into account.

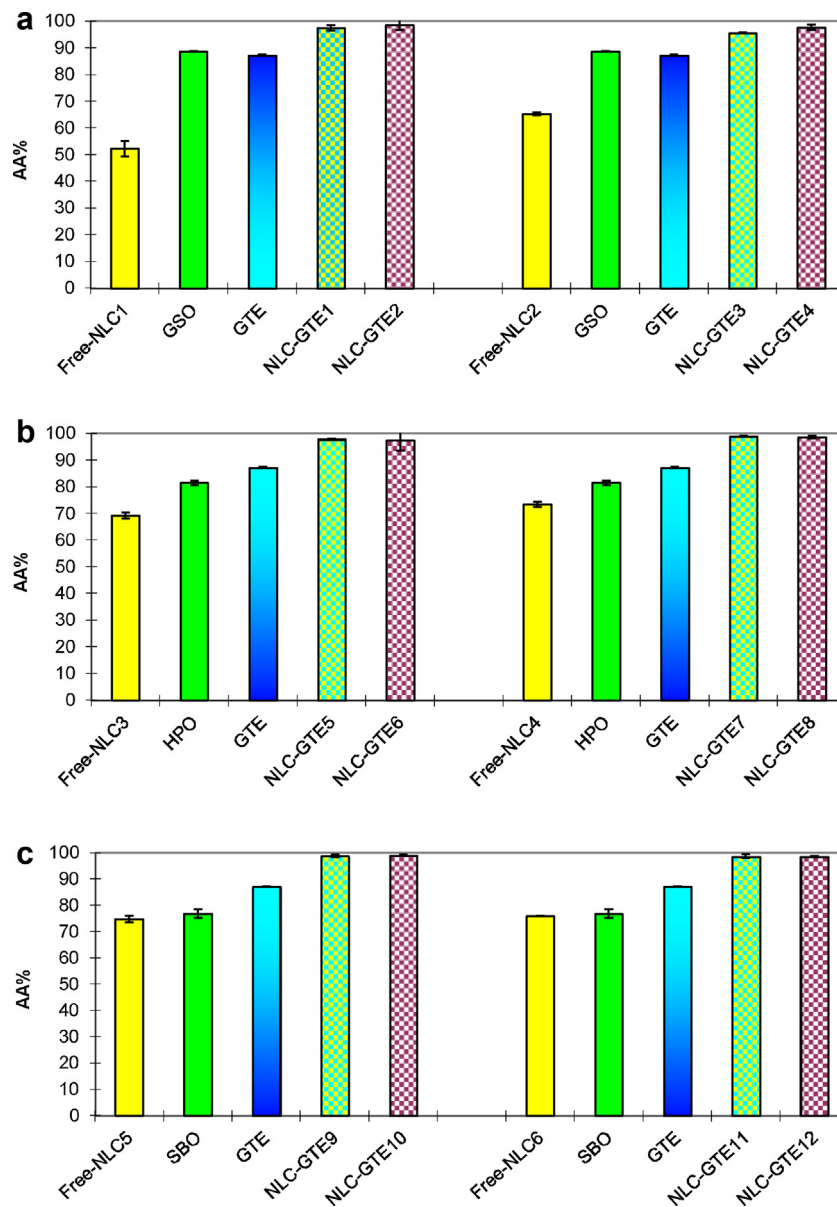


Fig. 6. Antioxidant activity of GTE-NLCs: a: NLCs prepared with GSO; b: NLCs prepared with HPO; c: NLCs prepared with SBO.

Considering all these aspects, the antioxidant capacity of NLCs–GTE samples may be related with the performance of complex lipid matrix by means of a synergy between lipid components. Indeed, the fatty acids from all the three kinds of vegetable oils used can act in synergy, thus, affecting the total AA of the obtained NLCs. In this way, it was demonstrated that the ability to capture free radicals from vegetable oils is higher than that of other individual antioxidants, because there are many available groups to neutralize them.

3.7. Antibacterial activity

Vegetable oils can be a rich source of antimicrobial agents [32]. For this reason, the NLCs–GTE samples were

tested for their ability to develop antimicrobial activity against *Escherichia coli*, which is a contamination indicator of food. The zone of inhibition was measured and expressed in millimeters. All of the experiments were performed in triplicate, and the results are reported as the average of these three experiments.

The representative results of antibacterial activity of NLCs–GTE against *Escherichia coli* are illustrated in Fig. 7.

The present investigations have shown a significant variation in the antibacterial activity of NLCs–GTE systems, which varies depending on the vegetable oils used and on the GTE concentration. Concerning the vegetable oils used for NLCs preparation, their antibacterial activity is increasing in the following order: SBO < GSO < HPO.

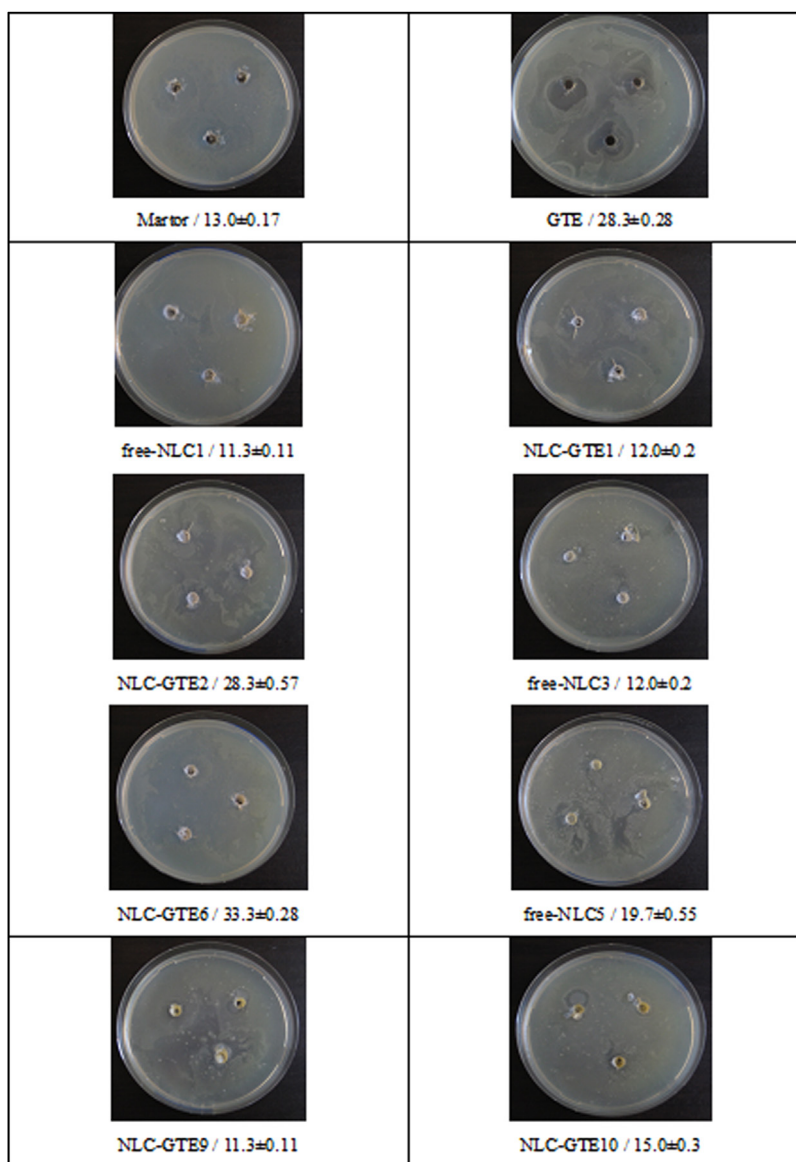


Fig. 7. Antibacterial activity of GTE–NLCs against *Escherichia coli* K 12-MG1655.

All tested NLCs–GTE samples were highly effective against *Escherichia coli*. It is evident from the present study that the obtained GTE–NLCs have good antimicrobial activity.

4. Conclusions

Green tea is a source of pharmacologically active molecules, an important member of the antioxidant food group, which provides a dietary source of biologically active compounds that help preventing a wide variety of diseases. Recent research identified green tea as Nature's gift for promoting human health [33]. Much interest was centered on the role of antioxidant activity with respect to the aging process and degenerative diseases, like cancer, cardiovascular diseases, and diabetes.

The results obtained by this study have demonstrated that the modified high shear homogenization method is suitable for the co-encapsulation of green tea extract together with other oils, such as grape seed oil, St. John's wort oil and sea buckthorn oil into different lipid nanomatrices. Concerning the effect of the two types of surfactants used, Tw20 and Tw80, on the mean particle size of NLCs, the smallest Zave was obtained for the NLCs prepared with Tw20. As referring to the GTE content, we observed that for all the three types of vegetable oils used, the smallest particle size was obtained for 0.1 wt% GTE content. Zeta potential evaluation of prepared GTE–NLCs nanodispersions has shown an excellent physical stability.

The evaluation of in vitro antioxidant properties has demonstrated that for all NLCs–GTE samples, the antioxidant activity was enhanced compared with that of

native GTE. The DSC results have shown that NLCs prepared with HPO or SBO and Tw20 lead to a less ordered crystalline arrangement, while their endothermic peaks are decreasing in intensity as compared with that of free NLCs. The antibacterial activity shows that GTE could be utilized as a good natural source of antioxidants and a possible food supplement or as an antimicrobial agent in pharmaceutical industry.

The process for the synthesis of NLCs at large scale using these readily available plants extracts has a potential commercial viability. It will help also to develop studies on the interface between biology and material science. By using such plant extracts, one can develop nanomedicines against various human and veterinary pathogens.

Acknowledgement

The work has been funded by the Sectoral Operational Programme Human Resources Development 2007–2013 of the Romanian Ministry of Labour, Family and Social Protection through the Financial Agreements POSDRU/107/1.5/S/76903.

References

- [1] P.D. Stapleton, S. Shah, J.C. Anderson, Y. Hara, J.M. Hamilton-Miller, P.W. Taylor, *Int. J. Antimicrob. Agents* 23 (5) (2004) 462.
- [2] K. Yoshino, Y. Hara, M. Sano, I. Tomita, *Biol. Pharm. Bull.* 17 (1994) 146.
- [3] G.M. Song, K.H. Lee, B.L. Seong, *Antivir. Res.* 68 (2005) 66.
- [4] Z.Y. Wang, S.J. Cheng, Z.C. Zhou, M. Athar, W.A. Khan, D.R. Bickers, H. Mukhtar, *Mutat. Res.* 223 (1989) 273.
- [5] W. Kim, M.H. Jeong, S.H. Cho, J.H. Yun, H.J. Chae, Y.K. Ahn, M.C. Lee, X. Cheng, T. Kondo, T. Murohara, J.C. Kang, *Circ. J.* 70 (2006) 1052.
- [6] J.V. Higdon, B. Frei, *Crit. Rev. Food Sci. Nutr.* 43 (2003) 89.
- [7] S. Kuriyama, T. Shimazu, K. Ohmori, N. Kikuchi, N. Nakaya, Y. Nishino, *JAMA* 296 (2006) 1255.
- [8] J. Nagano, S. Kono, D.L. Preston, K. Mabuchi, *Cancer Causes Control* 12 (2001) 501.
- [9] L. Zhong, M.S. Goldberg, Y.T. Gao, J.A. Hanley, M.E. Parent, F. Jin, *Epidemiology* 12 (2001) 695.
- [10] H. Tsuneki, M. Ishizuka, M. Terasawa, J.B. Wu, T. Sasaoka, I. Kimura, *Pharmacology* 4 (2004) 18.
- [11] G. Cao, E. Sofic, R.L. Prior, *J. Agr. Food Chem.* 44 (1996) 3426.
- [12] T. Masuda, Y. Inaba, T. Maekawa, Y. Takeda, H. Yamaguchi, K. Nakamoto, H. Kunitaga, S. Nishizato, A. Nonaka, *J. Agr. Food Chem.* 51 (2003) 1831.
- [13] N. Khan, H. Mukhtar, *Cancer Lett.* 269 (2009) 269.
- [14] I.F. Uchehgbu, S.P. Vyas, *Int. J. Pharm.* 172 (1998) 33.
- [15] M. Gulati, M. Grover, S. Singh, M. Singh, *Int. J. Pharm.* 165 (1998) 129.
- [16] D.D. Lasic, N.S. Templeton, *Adv. Drug Deliv. Rev.* 20 (1996) 221.
- [17] W.P. Bowe, J.B. Glick, A.R. Shalita, *Curr. Derm. Rep.* 1 (2012) 97.
- [18] T. Tschan, H. Steffen, A. Supersaxo, *Skin Pharmacol.* 10 (1997) 126.
- [19] C.C. Bettoni, C.C. Felippi, C. de Andrade, *J. Biomed. Nanotechnol.* 8 (2012) 258.
- [20] A.A. Attama, C.C. Müller-Goymann, *Colloids Surf A: Physicochem. Eng. Aspects* 315 (2008) 189.
- [21] I. Lacatusu, N. Badea, A. Murariu, N. Nichita, D. Bojin, A. Meghea, *Mol. Cryst. Liq. Cryst.* 523 (2010) 260.
- [22] P. Chan, J.T. Cheng, C.W. Tsao, C.S. Niu, C.Y. Hong, *Life Sci.* 59 (1996) 2067.
- [23] C. Ungureanu, M. Ferdeş, *Chem. Eng. Trans.* 20 (2010) 223.
- [24] W. Mehnert, K. Mäder, *Adv. Drug. Deliv. Rev.* 47 (2001) 165.
- [25] T.H. Wu, F.L. Yen, L.T. Lin, T.R. Tsai, C.C. Lin, T.M. Cham, *Int. J. Pharm.* 346 (2008) 160.
- [26] R.H. Müller, M. Radtke, S.A. Wissing, *Int. J. Pharm.* 242 (2002) 121.
- [27] H. Bunjes, *Curr. Opin. Colloid Interface Sci.* 16 (2011) 405.
- [28] J.W. Hageman, M. Dekker, *NY U S A* (1988) 29.
- [29] K. Sato, *Chem. Eng. Sci.* 56 (2001) 2255.
- [30] H. Bunjes, K. Westesen, H.J.K. Michel, *Int. J. Pharm.* 129 (1996) 159.
- [31] V.S. Kumaran, K. Arulmathi, P. Kalaiselvi, *Basic Nutr. Invest.* 25 (2009) 847.
- [32] M. Ferdes, C. Ungureanu, *UPB Sci. Bull. Series B* 74 (2) (2012) 87.
- [33] N. Khan, H. Mukhtar, *Life Sci.* 81 (2007) 519.